PSYCHOLOGICAL SCIENCE

# Hyperexcitation of ovBNST CRF neurons during stress contributes to female-biased expression of anxiety-like avoidance behaviors

**Na Zhang[1,2]†, Sha Zhao[1]†, Yanqiao Ma[1]†, Zhixin Xiao[1], Bao Xue[1], Yuan Dong[1], Qingyu Wang[3], Huamin Xu[1], Xia Zhang[1]*, Ying Wang[1,4]***



**Corticotropin releasing factor (CRF) network in the oval nucleus of bed nuclei of the stria terminalis (ovBNST) is generally indicated in stress, but its role in female-biased susceptibility to anxiety is unknown. Here, we established a female-biased stress paradigm. We found that the CRF release in ovBNST during stress showed female-biased pattern, and ovBNST CRF neurons were more prone to be hyperexcited in female mice during stress in both in vitro and in vivo studies. Moreover, optogenetic modulation to exchange the activation pattern of ovBNST CRF neurons during stress between female and male mice could reverse their susceptibility to anxiety. Last, CRF receptor type 1 (CRFR1) mediated the CRF-induced excitation of ovBNST CRF neurons and showed female-biased expression. Specific knockdown of the CRFR1 level in ovBNST CRF neurons in female or overexpression that in male could reverse their susceptibility to anxiety. Therefore, we identify that CRFR1-mediated hyperexcitation of ovBNST CRF neurons in female mice encode the female-biased susceptibility to anxiety.**

## INTRODUCTION

Anxiety is one of the most common mental disorders worldwide, and its incidence has been further increased as the outbreak of COVID-19 pandemic (*1*), while current anti-anxiety therapies remain ineffective for a large proportion of patients (*2*, *3*). It has been well characterized that anxiety disorders are more prevalent in women, as approximately twice than in men (*4*). However, the biological mechanisms that contribute to the sex difference in anxiety are still poorly understood, partly due to the male-biased choice in most neuroscience experiments to avoid the impact of tricky hormone surges across estrous cycles in females (*5*, *6*). Therefore, identifying the key neural network for regulating sex differential vulnerability to anxiety is indispensable for treatment and prevention, which would have enormous clinical and societal impact.

Many complexities, including brain regions or hormonal changes, are involved in anxiety, which might construct the network accounting for the sex difference in anxiety (*4*, *7*–*9*). Corticotropin releasing factor (CRF) is a generally acknowledged stress hormone (*10*). Behavioral studies have demonstrated that the CRF hormone system is essential for coordinating the adaptive response to stressful situations, and its excessive activation is critically involved in the etiology of anxiety (*11*). The oval nucleus of the bed nuclei of the stria terminalis (ovBNST) is a critical site of action for CRF and has been suggested as a node in stress and anxiety-related network (*12*). Stressful and anxiogenic stimuli could result in the release of CRF in ovBNST, principally originating from the lateral division of the central amygdala (CeA) (*13*) and subsequently acts through CRF receptor type 1 (CRFR1) on ovBNST neurons (*14*). Moreover, ovBNST itself is also rich in CRF-containing neurons (*15*), optogenetically increasing ovBNST neural activities promoted several independent anxious state features (*12*). However, although it is believed that CRF neurotransmission in the ovBNST mediates the expression of anxiety, our understanding of the role of the ovBNST network in sex-specific behaviors remains unknown.

BNST is one of the most famous sexually dimorphic regions in both humans and animals (*16*, *17*). As the dorsal lateral part of the BNST, ovBNST also showed sexual dimorphism with its CRF neurons in females outnumbering that in males in both rats and mice (*18*–*20*). However, these studies focused on sexual differences of ovBNST CRF neurons in anatomy but not their network functions. Therefore, we were interested in establishing female-biased stress protocols and using it to probe the role of the ovBNST CRF network in encoding the sex-specific susceptibility to anxiety. It has been reported that chronic physical and social isolation stress could induce sex-specific consequences in anxiety-like behaviors (*21*, *22*), but the performance of acute stress remains uncovered. Here, we introduced forced swimming as an acute strong stress (*23*) and successfully induced female-biased vulnerability to anxiety-like behaviors. Using this model, we unexpectedly found that CeA afferents in the ovBNST did not show notable contributions to sex differences in anxiety behavior but that preexisting sex differences in the function of CRFR1 and the activation pattern of CRF neurons in ovBNST during acute stress exposure drive sex differential vulnerability to anxiety. These results suggest that the pre-existing sexual differences in the ovBNST CRF network shape the initial development of female-biased susceptibility to anxiety, providing a potential therapeutic target for early intervention across sex and promoting the translation to human health.

## RESULTS

### Female mice display higher susceptibility to anxiety than male mice

Stress is a major risk factor for anxiety (*21*). Female and male C57BL/6J mice were exposed to forced swimming stress. Then, we tested anxiogenic effects of these stress stimuli 24 hours later by

[1]Institute of Neuropsychiatric Diseases, The Affiliated Hospital of Qingdao University, Qingdao University, Qingdao 266071, China. [2]Qingdao Hospital, University of Health and Rehabilitation Sciences (Qingdao Municipal Hospital), Qingdao 266000, China. [3]Department of Anesthesiology, The Affiliated Hospital of Qingdao University, Qingdao 266000, China. [4]Program in Cellular and Molecular Medicine, Boston Children's Hospital, Boston, MA 02115, USA.
*Corresponding author. Email: ying.wang@childrens.harvard.edu (Y.W.); xia.zhang@qdu.edu.cn (X.Z.)
†These authors contributed equally to this work.

using two standard behavioral assays: the open-field test (OFT) and elevated plus maze (EPM) test (Fig. 1A and fig. S1A). To verify whether ovarian hormones affect behaviors, we divided female mice into estrus stage (including proestrus, estrus, and metestrus) and diestrus stage by vaginal cytology (fig. S1B). Female mice, either in estrus or diestrus stage, exposed to 5-min and 10-min forced swimming both spent less time in the center zone or the open arm than the respective control animals but not 3 min (fig. S1, C to H). While male mice only exposed to 10-min forced swimming spent less time in the center zone or the open arm than the respective control animals but not 3 min and 5 min (fig. S2, A to F). Because there is no significant difference between estrus and diestrus stage, therefore, to avoid the additional stress imposed by the vaginal smear procedure, we duplicated the test for the anxiogenic effects of 5-min forced swimming stress in both female and male mice without vaginal cytology (Fig. 1A). The results showed that 24 hours after 5-min forced swimming stress, only female, but not male, mice showed avoidance behaviors in OFT and EPM with less time spent in the center zone or the open arm than the respective control animals (Fig. 1, B to G). These results indicated that forced swimming stress could induce interesting female-biased susceptibility to anxiety, with female mice developing increased avoidance behaviors in OFT and EPM following shorter stress durations. Moreover, with sufficient stress, both sexes exhibit behavioral susceptibility, rendering this is a useful model for studying the sex differential susceptibility to anxiety. The above results indicate that the estrus cycle does not produce significant effects with the response to acute strong stress in female mice, and 5-min forced swimming stress is a useful paradigm to study the female-biased susceptibility to anxiety.

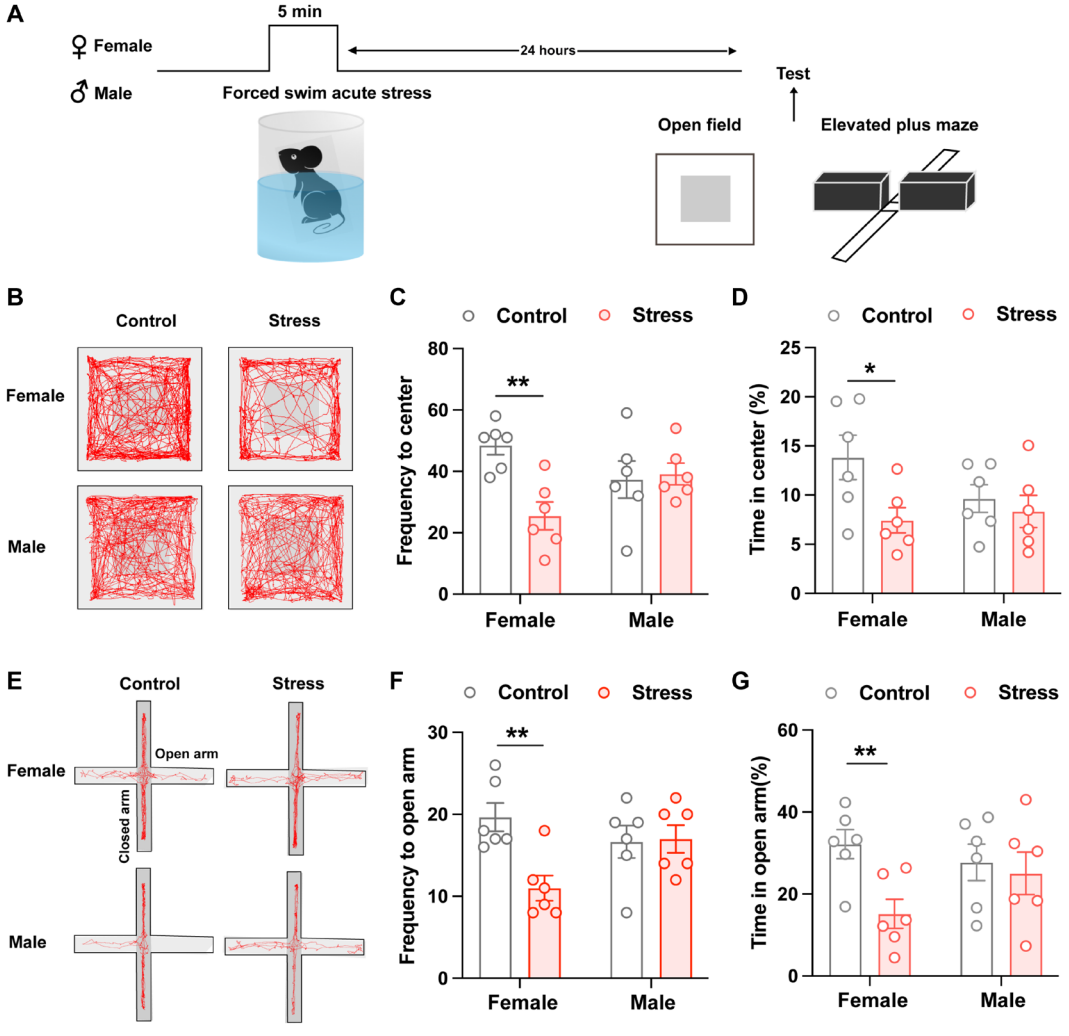


**Fig. 1. Female mice display higher susceptibility to anxiety than male mice after acute exposure to forced swimming stress.** (**A**) Experimental timeline for measuring anxiety-like behaviors following 5-min treatment of forced swimming. (**B**) Locomotion traces for representative control and forced swimming-exposed female and male mice in EPM. Light gray marks closed arms. (**C** and **D**) Quantification of frequency to open arms (C) and percentage time spent in the open arms (D) of EPM in female and male mice (*$P$ < 0.05 and **$P$ < 0.01, unpaired $t$ test). (**E**) Locomotion traces for representative control and forced swimming-exposed female and male mice in OFT. Light gray square marks the designated center zone. (**F** and **G**) Quantification of frequency to center zone (F) and percentage time spent in the center zone (G) of OFT in female and male mice (**$P$ < 0.01, unpaired $t$ test).

### CeA CRF projections to the ovBNST mediate stress-induced anxiety in both sexes

It has been reported that stressful and anxiogenic stimuli could result in the release of CRF in ovBNST, which primarily acts on the CRFR1 (*14*). Meanwhile, the ovBNST itself is also rich in CRF-containing neurons (*15*). Therefore, CRF afferents, CRFR1, and CRF neurons together constitute the CRF network in the ovBNST. Then, we attempted to explore whether the expression and activity of the CRF network in ovBNST contribute to the sex susceptibility to anxiety. Because ovBNST primarily receives CRF afferents from the lateral CeA, we examined the structural connectivity from CeA CRF neurons to ovBNST CRF neurons with an anterograde monosynaptic tracing virus AAV2/1-Ef1α-DIO-EGFP-WPRE injected into the CeA and AAV2/9-Ef1α-DIO-mCherry-WPRE into the ovBNST of CRF-Cre mice (Fig. 2A). We found that CeA CRF neurons was anterogradely connected with ovBNST CRF neurons (Fig. 2B), and nearly 50% percent of ovBNST CRF neurons were innervated by CeA CRF neurons in both sexes (Fig. 2C). We then performed in vivo fiber photometry (Fig. 2D) (*24*) to monitor the activity of CeA-ovBNST CRF projections during forced swimming stress separately in female and male mice. The genetically encoded $Ca^{2+}$ indicator GCaMP6m was specifically expressed in the CeA CRF neurons by stereotactically injecting AAV2/9-Ef1α-DIO-GCaMP6(m)-WPRE into the CeA of *CRF-Cre* mice (Fig. 2E). Extensive CeA CRF terminals were observed in the ovBNST, and the photometry fiber was implanted above the terminals in the ovBNST (Fig. 2E). We found that the activity of CeA-ovBNST CRF projections, indicated by the $\Delta F/F_0$, was increased during forced swimming stress without sex differences (Fig. 2, F and G). Representative traces of calcium signals for forced swimming application in female and male were shown as Fig. 2F.

To further investigate whether CeA CRF projections within the ovBNST are important for stress-induced anxiety, we introduced two paradigms. First, we expressed AAV2/9-Ef1α-DIO-ChR2-WPRE or AAV2/9-Ef1α-DIO-eNpHR-WPRE in CeA CRF neurons and targeted optical fibers to the ovBNST for delivery of a blue (473 nm, 20 Hz, 10 ms, 10 mW, 5 min) or yellow (561 nm, continuous, 10 mW, 5 min) laser to specifically activate or inhibit CeA CRF projections within the ovBNST during OFT and EPM behavior tests. The results showed that optogenetic activation of CeA CRF projections within the ovBNST reduced the frequency and percentage of open arm entries on the EPM and center zone entries on the OFT in both sexes, while optogenetic inhibition of CeA CRF projections within the ovBNST did not affect the condition of open arm entries on the EPM and center zone entries on the OFT in females but increased the durations in center zone in males (fig. S3, A to D). However, these experiments were conducted without forced swimming stress. To further explore the effects of activating or silencing the CeA-ovBNST CRF projections both during and after stress, we introduced chemogenetics. We expressed AAV2/9-Ef1α-DIO-hM3D-WPRE or AAV2/9-Ef1α-DIO-hM4D-WPRE in CeA CRF neurons and targeted cannulas to the ovBNST for intra-ovBNST administration of CNO 10 min before forced swimming stress to specifically activate or inhibit CeA CRF projections within the ovBNST during and after stress (Fig. 2, H and I). The results showed that activating the CeA-ovBNST CRF projections both during and after stress could increase stress-induced avoidance behaviors in OFT and EPM with reduced frequency and percentage of open arm entries and center zone entries in both male and female mice (Fig. 2, J to M). Then, silencing the CeA-ovBNST CRF projections both during and after stress could decrease stress-induced avoidance behaviors in OFT and EPM with increased frequency and percentage of open arm entries and center zone entries in both male and female mice (Fig. 2, J to M). These results demonstrated that the activity of CRF afferents within the ovBNST mediates stress and anxiety in both sexes without significant sex differences. The above results suggest that there were no sexual differences in the anatomy of CeA-ovBNST CRF pathway as well as their role in stress-induced susceptibility to anxiety.

### Overall CRF release in ovBNST is sexual different during stress and drives hyperexcitation of ovBNST CRF neurons in female mice in vitro

To further identify the condition of overall CRF release in ovBNST during stress, we introduced the CRF sensor to monitor the dynamic CRF release in ovBNST during forced swimming in both females and males (*25*). We expressed AAV9-hsyn-DIO-CRF2.0 into the ovBNST in *CRF-Cre* mice (Fig. 3A). The results showed that the overall CRF release in ovBNST during forced swimming stress showed notable sexual differences. Although there was significant increase of CRF release in the first 100s in both female and male mice, only female mice showed another increase peak of CRF release in the following 200s, but not male mice (Fig. 3B). These results indicate that in addition to CeA CRF afferents, there might be other presynaptic release of CRF in ovBNST or local release of CRF from ovBNST CRF interneurons, which lead to the sexual different CRF release pattern in ovBNST during stress.

Then, we tried to test the effect of CRF release on the activity of ovBNST CRF neurons in in vitro experiments. Using whole-cell electrophysiological recordings in ovBNST CRF neurons labeled by green fluorescent protein (Fig. 3C), we firstly compared the spontaneous firing rate of ovBNST CRF neurons between control mice and stressed mice. The results showed that, in control mice, the firing rate of ovBNST CRF neurons was lower in female than male (Fig. 3, D and E). However, in stressed mice, the firing rate of ovBNST CRF neurons was increased in both sexes with females showing a prominent increase to reach the same levels of males (Fig. 3, D and E). Moreover, we also compared the condition before and after CRF exposure which mimic the stress condition. We found that there were notable sex differences in spontaneous action potential and evoked action potential. In base condition, ovBNST CRF neurons showed greater excitation in males with higher spontaneous action potential (Fig. 3, F and G) and evoked action potential (Fig. 3, I and J). However, after exposure to CRF, which mimics the stress condition, both spontaneous action potential and evoked action potential in ovBNST CRF neurons of both males and females increased with females showing a prominent increase, as compared to base condition (Fig. 3, F to K). Moreover, the frequency and amplitude of spontaneous excitatory postsynaptic currents (sEPSCs) were in the same level between sexes in control condition (Fig. 3L). The frequency, but not amplitude, of sEPSC was significantly higher in females than males after exposure of CRF (Fig. 3M) or in stressed mice (Fig. 3N). These results suggest that ovBNST CRF neurons were more prone to be activated in female mice than male mice during exposure to CRF-dependent stress.

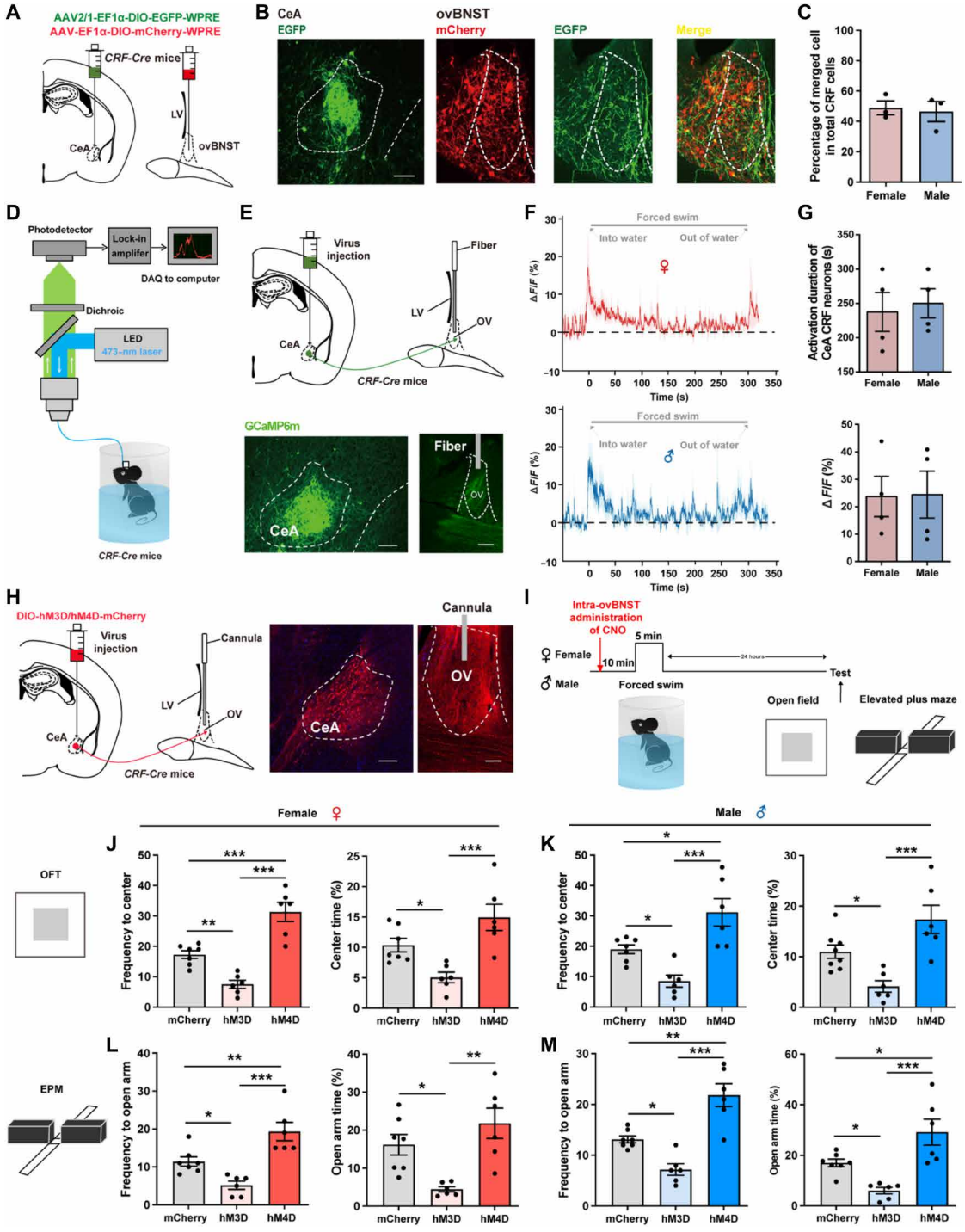


**Fig. 2. CeA CRF projections to the ovBNST mediate stress and anxiety in both sexes.** (**A**) Schematic diagram of dual viral injections into the ovBNST and CeA of *CRF-Cre* mice for anterograde monosynaptic tracing. (**B**) A part of mCherry$^{+}$ CRF neurons in the ovBNST were labeled with EGFP. Scale bar, 200 μm. (**C**) Quantification of the percentage of merged cell in total CRF cells. (**D**) Experimental setup for fiber photometry. (**E**) Top: Virus injection and fiber configuration. Bottom: Representative image showing expression of GCaMP6m in CeA and ovBNST. Scale bars, 200 μm. (**F**) Example trace of calcium signals for forced swimming application in female (top) and male (bottom) mice. (**G**) Quantification of forced swimming-induced activation duration (top) and peak Δ*F*/*F* (%) (bottom) for female and male mice. (**H**) Left: Virus injection and cannula configuration. Right: Representative image showing expression of hM3D/hM4D-mCherry in CeA and terminals in ovBNST. Scale bars, 200 μm. (**I**) Experimental timeline. (**J** and **K**) Quantification of frequency to center zone and percentage time spent in the center zone of OFT in female (J) and male (K) mice [$^{*}P < 0.05$, $^{**}P < 0.01$, and $^{***}P < 0.001$, one-way analysis of variance (ANOVA) and post hoc test]. (**L** and **M**) Quantification of frequency to open arm and percentage time spent in the open arm of EPM in female (L) and male (M) mice ($^{*}P < 0.05$, $^{**}P < 0.01$, and $^{***}P < 0.001$, one-way ANOVA and post hoc test). LED, light-emitting diode; DAQ, data acquisition; OV, oval nucleus; CeA, central amygdala; LV lateral ventricle.

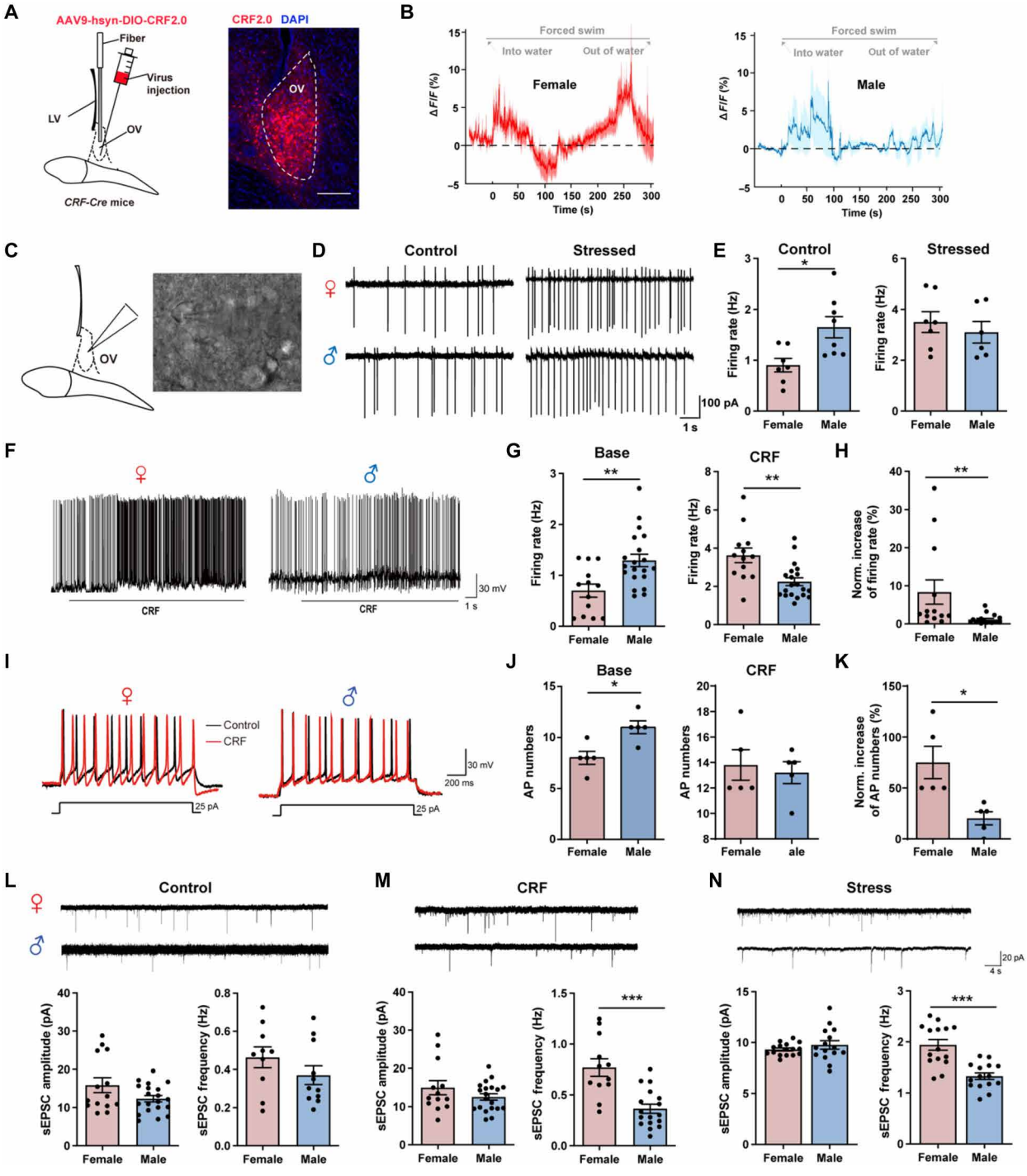


**Fig. 3. CRF release is sexual different in ovBNST during stress and drives hyperexcitation of ovBNST CRF neurons in female mice in vitro.** (**A**) Left: Virus injection. Right: Representative image showing expression of CRF2.0 in ovBNST. Scale bar, 200 μm. (**B**) Example trace of CRF release in ovBNST during forced swimming stress in female (left) and male (right) mice. (**C**) Schematic of whole-cell patch-clamp recordings of ovBNST neurons. (**D**) Representative firing rate of ovBNST CRF neurons before and after stress in female (up) and male (down) mice. (**E**) Quantification of the firing rate of ovBNST CRF neurons before (left) and after (right) stress (*$P < 0.05$, Student's *t* test). (**F**) Representative firing frequency of ovBNST neurons after perfusion of CRF in female (left) and male (right) mice. (**G**) Quantification of the firing rate before (left) and after (right) CRF perfusion in female and male mice (**$P < 0.01$, Student's *t* test). (**H**) Quantification of the normalized increase of firing rates after CRF perfusion in female and male mice (**$P < 0.01$, Student's *t* test). (**I**) Representative evoked firing activity was recorded before and after perfusion of CRF in female (top) and male (bottom) mice. (**J**) Quantification of the evoked AP numbers before (left) and after (right) CRF perfusion in female and male mice (*$P < 0.05$, Student's *t* test). (**K**) Quantification of the normalized increase of evoked AP numbers after CRF perfusion in female and male mice (*$P < 0.05$, Student's *t* test). (**L** to **N**) Example sEPSC traces of ovBNST CRF neurons and quantitative analysis of sEPSC amplitude and frequency in control (L), after CRF perfusion (M) and after stress (N) in female and male mice (***$P < 0.001$, Student's *t* test). DAPI, 4′,6-diamidino-2-phenylindole.

### Stress induces in vivo hyperexcitation of ovBNST CRF neurons in female mice

Then, we tested whether ovBNST CRF neurons were more prone to be activated during forced swimming exposure in female mice in vivo. We performed fiber photometry to monitor the activity of ovBNST CRF neurons during forced swimming stress in female and male mice (Fig. 4A). The genetically encoded $Ca^{2+}$ indicator GCaMP6m was specifically expressed in ovBNST CRF neurons by injecting AAV2/9-Ef1α-DIO-GCaMP6(m)-WPRE into the ovBNST of *CRF-Cre* mice (Fig. 4B). We found that although the initial activation shown in the male trace appears to be of a higher amplitude than the female trace, the activation of ovBNST CRF neurons in females was persistent throughout the whole 5-min process while in males was transient for approximately 2 min (Fig. 4, C to E). Moreover, we also showed the data of ovBNST CRF neuronal calcium signals in both sexes subjected to 10-min forced swim stress (fig. S4), and we used dashed lines to indicate 3, 5, and 10 min during the whole process for forced swimming stress (fig. S4, B and C). The results showed that in the first 3 min, there were no significant differences of ovBNST CRF neuronal calcium signals in both sexes, which was consistent to the results that both sexes did not show increased anxiety after 3-min forced swim stress. However, from 3 to 5 min, there was an increase of calcium signals in female, but not male, ovBNST CRF neurons, which might result in the female-biased expression of anxiety-like behaviors after 5-min forced swim stress. Then, from 5 to 10 min, the calcium signals of female ovBNST CRF neurons were still above the baseline, and there was also an increase of calcium signals in male ovBNST CRF neurons, which might result in the increased anxiety in both sexes after 10-min forced swim stress. These results suggest that hyperexcitation of ovBNST CRF neurons in females is associated with the female-biased expression of anxiety.

ovBNST CRF neurons have been reported to be sexual dimorphic in rodents, and we also found that ovBNST CRF neurons in female mice significantly outnumbered those in male mice (fig. S5, A and B) which is in consistent with previous studies (*18*). Moreover, specific activation of ovBNST CRF neurons was sufficient to induce anxiety-like behaviors, while inhibition of ovBNST CRF neurons did not significantly affect anxiety-like behaviors in both sexes (fig. S6). However, it is not clear whether the role of ovBNST CRF neurons in stress-induced anxiety shows sexual dimorphism. To further illustrate the importance of ovBNST CRF neurons in female-biased susceptibility to anxiety, we injected AAV2/9-EF1a-DIO-Caspase3 into the ovBNST to ablate the ovBNST CRF neurons in *CRF-Cre* female and male mice (Fig. 4F). After exposure to forced swim stress, the frequency and percentage of open arm entries in EPM were reversed to control level after ablation of ovBNST CRF neurons (Fig. 4, G to J). However, ablation of ovBNST CRF neurons in male mice did not affect the avoidance behaviors when compared to control group or stress + mCherry group (Fig. 4, K to N). The above results confirmed that ovBNST CRF neurons are involved in the development of stress-induced anxiety in female but not male mice.

To further verify whether the hyperexciation of CRF neurons in ovBNST accounts for the female-biased sensitivity to forced swimming stress, we introduced optogenetic strategies (Fig. 5A). First, Cre recombinase–dependent expression of ChR2 or eNpHR3.0 was achieved by injecting AAV-Ef1a-DIO-ChR2-mCherry or AAV-Ef1a-DIO-eNpHR3.0-mCherry into the ovBNST of *CRF-Cre* female and male mice (Fig. 5B). Then, we set different optogenetic activation/inhibition patterns to mimic the observed activation patterns of ovBNST CRF neurons during stress in Fig. 4C, where there was an increase of ovBNST CRF neuronal activities from 100s to 300s during forced swimming in females but a decrease in males. Therefore, only from 100s to 300s, but not the whole process, during forced swimming, we optogeneticlly manipulated the activity of ovBNST CRF neurons in females or males. The results showed that optogenetic inhibition of ovBNST CRF neurons from 100s to 300s during 5-min forced swimming in female mice could prevent the expression of stress-induced anxiety-like behaviors with increased frequency and duration of open arm entries and center zone entries, that is to make female behave like male mice (Fig. 5, C to F). While optogenetic activation of ovBNST CRF neurons from 100s to 300s during 5-min forced swimming in male mice could promote the expression of the stress-induced anxiety-like behaviors with reduced frequency and duration of open arm entries and center zone entries, that is to make male behave like females (Fig. 5, G to J).

These results suggest that the sex difference in activation patterns of ovBNST CRF neurons plays an important role in the female-biased susceptibility to forced swimming stress. Optogenetic modulation to exchange the activation pattern of ovBNST CRF neurons during stress between female and male mice could reverse their susceptibility to stress-induced anxiety.

### CRFR1 mediates the hyperexcitation of ovBNST CRF neurons and contributes to the female-biased susceptibility to anxiety

The above results demonstrated that the hyperexcitation of ovBNST CRF neurons driven by CRF release during stress in female mice contributed to the expression of female-biased anxiety-like behaviors. It is generally acknowledged that CRF primarily acts on the CRFR1. CRFR1 is a postsynaptic $G_s$-coupled receptor and could mediate the release of intracellular calcium from stores (*26*). Then, we speculate that CRFR1 might mediate the CRF-induced excitation of ovBNST CRF neurons in a sex-specific manner, which further generate sexual dimorphism in stress-induced anxiety.

First, we examined the expression of CRFR1 in ovBNST with the Western blot. The prestress expression of ovBNST CRFR1 in female mice significantly outnumbered that in male mice (Fig. 6A). To test whether CRFR1s in the ovBNST generally modulate the generation of sex-specific susceptibility to stress-induced anxiety, traditional pharmacological manipulation was used. We administrated the selective CRFR1 antagonist R121919 (*27*) into the ovBNST in female or male mice before 5-min forced swimming stress (fig. S7, A and B). Behavioral results showed that R121919 prevented the expression of anxiety-like behaviors in female mice exposed to 5-min forced swimming stress while further reduced the avoidance behaviors in male mice (fig. S7, C to J). In contrast, intra-ovBNST administration of the CRFR1 agonist CRF before 5-min forced swimming could further increase the stress-induced avoidance behaviors in female mice and promote the expression of anxiety in male mice (fig. S7, K to R). Moreover, intra-ovBNST administration of R121919 significantly decreased the susceptibility to anxiety in male mice with 10-min forced swimming stress, while CRF significantly enhanced the susceptibility to anxiety in female mice with 3-min forced swimming stress (fig. S8). These results indicate that the ovBNST CRFR1 is a crucial factor for the generation of sex-specific susceptibility to anxiety in both sexes.

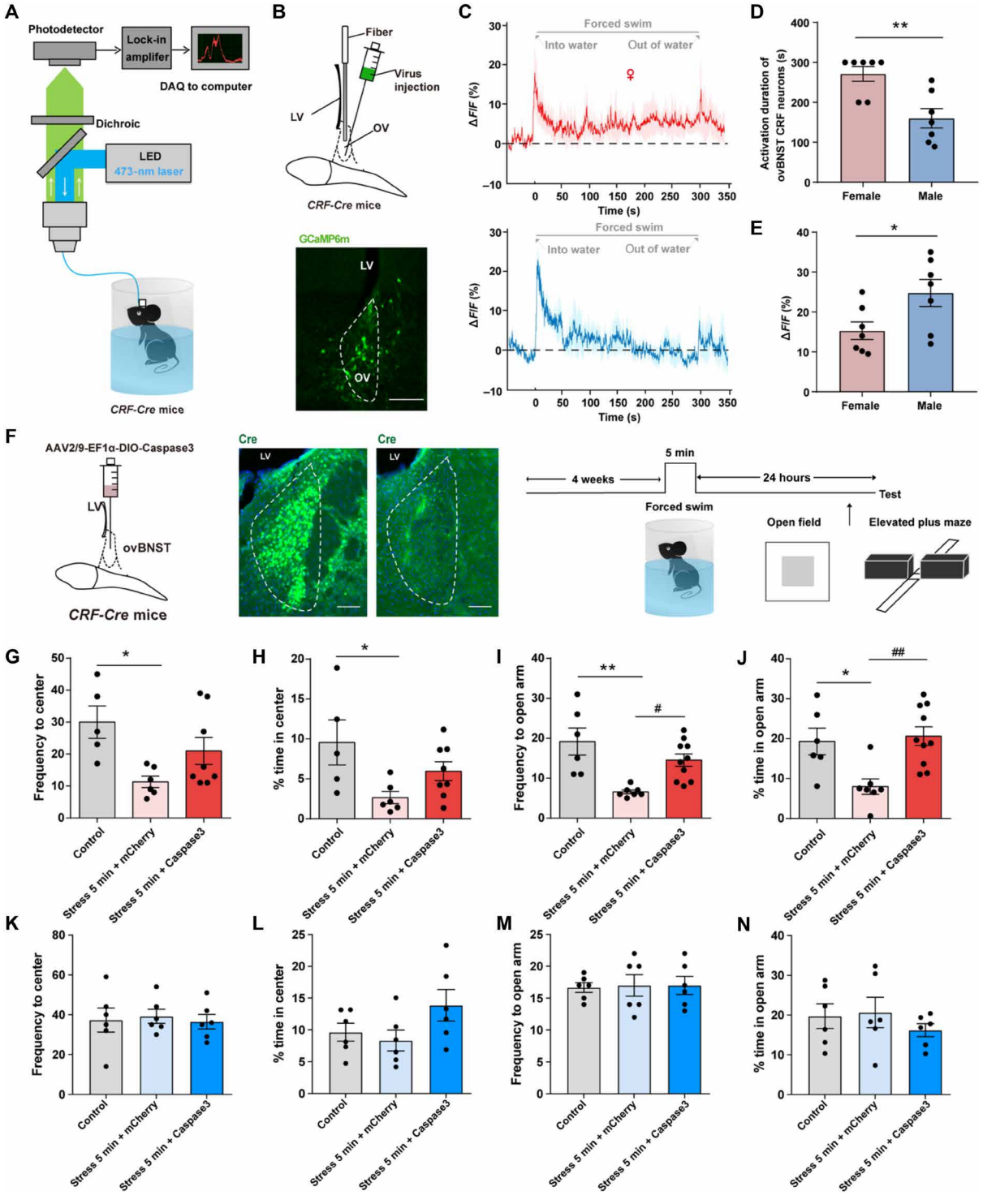


**Fig. 4. Hyperexcitation of ovBNST CRF neurons during stress contribute to female-biased expression of anxiety.** (**A**) Experimental setup for fiber photometry. (**B**) Top: Virus injection and fiber configuration. Bottom: Representative image showing expression of GCaMP6m in ovBNST. Scale bar, 200 μm. (**C**) Example trace of ovBNST CRF neuronal calcium signals during forced swimming stress in female (top) and male (bottom) mice. (**D** and **E**) Comparison of forced swimming-induced activation duration of ovBNST CRF neurons (D) and peak Δ*F*/*F* (%) (E) between female and male mice (**P* < 0.05 and ***P* < 0.01, Student's *t* test). (**F**) Left: Schematic diagram of ablation of ovBNST CRF neurons with intra-ovBNST injection of AAV-flex-taCasp3 in *CRF-Cre* female mice. Right: Immunostaining of Cre expression in a CRF::mCherry mouse and a CRF::Cas-3 mouse. Scale bars, 200 μm. (**G** and **H**) Quantification of frequency to center zone (G) and percentage time spent in the center zone (H) of OFT in female mice (**P* < 0.05, one-way ANOVA and post hoc test). (**I** and **J**) Quantification of frequency to open arm (I) and percentage time spent in the open arm (J) of EPM in female male mice (**P* < 0.05, ***P* < 0.01, $^{\#}P$ < 0.05, and $^{\#\#}P$ < 0.01, one-way ANOVA and post hoc test). (**K** and **L**) Quantification of frequency to center zone (K) and percentage time spent in the center zone (L) of OFT in male mice. (**M** and **N**) Quantification of frequency to open arm (M) and percentage time spent in the open arm (N) of EPM in male mice.

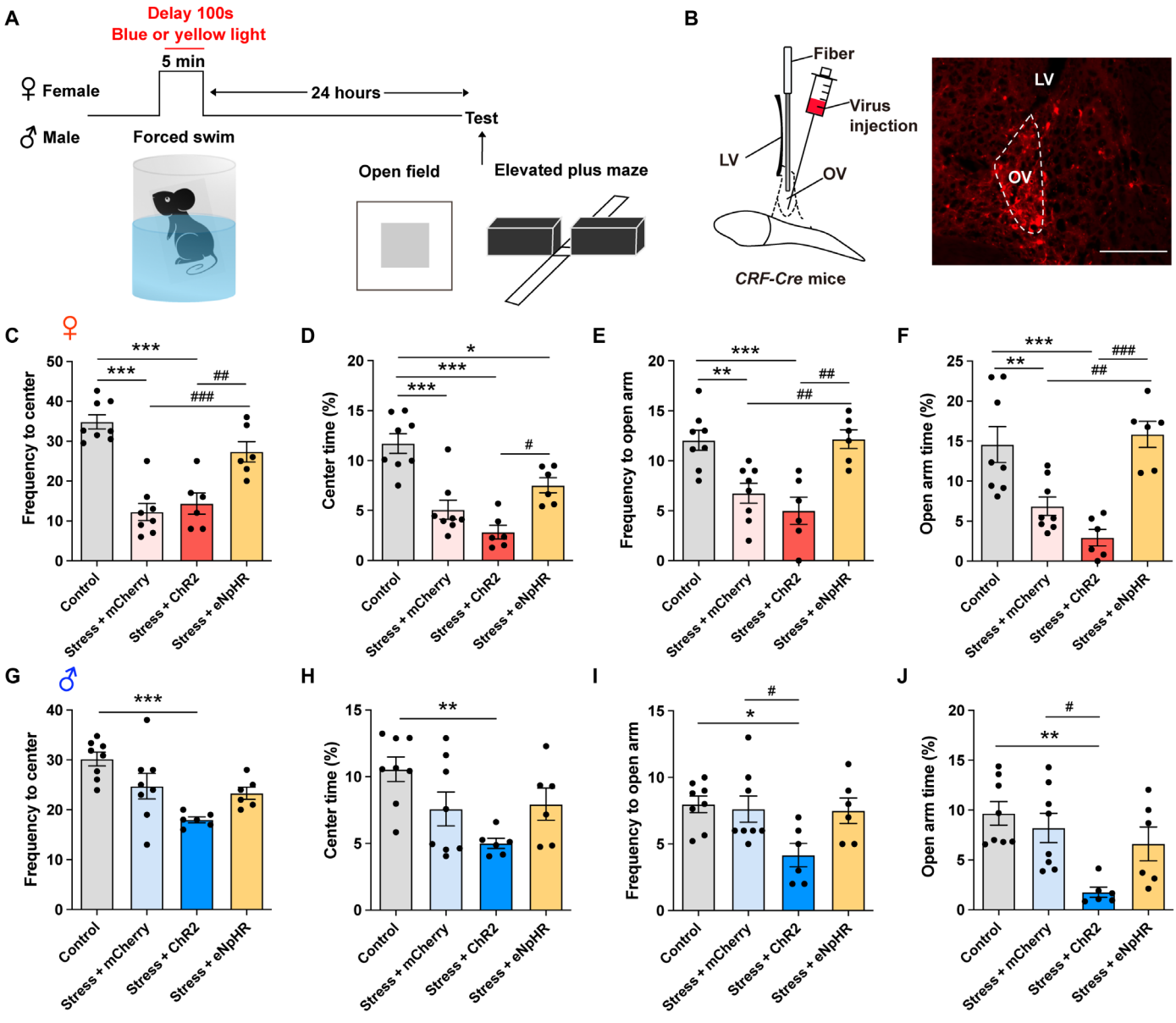


**Fig. 5. Optogentic manipulation to exchange the activation pattern of ovBNST CRF neurons during stress between female and male mice could reverse their susceptibility to anxiety.** (**A**) Experimental timeline. (**B**) Left: Virus injection and fiber configuration. Right: Representative image showing expression of ChR2-mCherry in ovBNST. Scale bar, 200 μm. (**C** and **D**) Quantification of frequency to center zone (C) and percentage time spent in the center zone (D) of OFT in female mice (*$P < 0.05$, ***$P < 0.001$, $^{\#}P < 0.05$, $^{\#\#}P < 0.01$, and $^{\#\#\#}P < 0.001$, one-way ANOVA and post hoc test). (**E** and **F**) Quantification of frequency to open arm (E) and percentage time spent in the open arm (F) of EPM in female mice (**$P < 0.01$, ***$P < 0.001$, $^{\#\#}P < 0.01$, and $^{\#\#\#}P < 0.001$, one-way ANOVA and post hoc test). (**G** and **H**) Quantification of frequency to center zone (G) and percentage time spent in the center zone (H) of OFT in male mice (**$P < 0.01$ and ***$P < 0.001$, one-way ANOVA and post hoc test). (**I** and **J**) Quantification of frequency to open arm (I) and percentage time spent in the open arm (J) of EPM in male mice (*$P < 0.05$, **$P < 0.01$, and $^{\#}P < 0.05$, one-way ANOVA and post hoc test).

However, traditional pharmacological manipulation is a non-cell type–specific method. Therefore, we need to further identify the role of CRFR1 in specific ovBNST CRF neurons. First, the immunohistochemistry results showed that ovBNST CRF neurons are colabeled with CRFR1 in both sexes (Fig. 6, B and C). Then, the in vitro electrophysiological recordings in ovBNST CRF neurons showed that CRF perfusion–induced excitation of ovBNST CRF neurons could be blocked by the CRFR1 antagonist, R121919, in both sexes (Fig. 6, D and E). These results indicated that CRFR1 could modulate CRF-induced excitation of ovBNST CRF neurons. Last, we modulated the expression of CRFR1 in ovBNST CRF neurons to test whether the CRFR1 contributed to the female-biased susceptibility to stress-induced anxiety (Fig. 6F). As the expression of CRFR1 in ovBNST is higher in females than males, we expressed the virus DIO-mCherry-shRNA3(CRFR1) into the ovBNST to knock down the expression of CRFR1 in

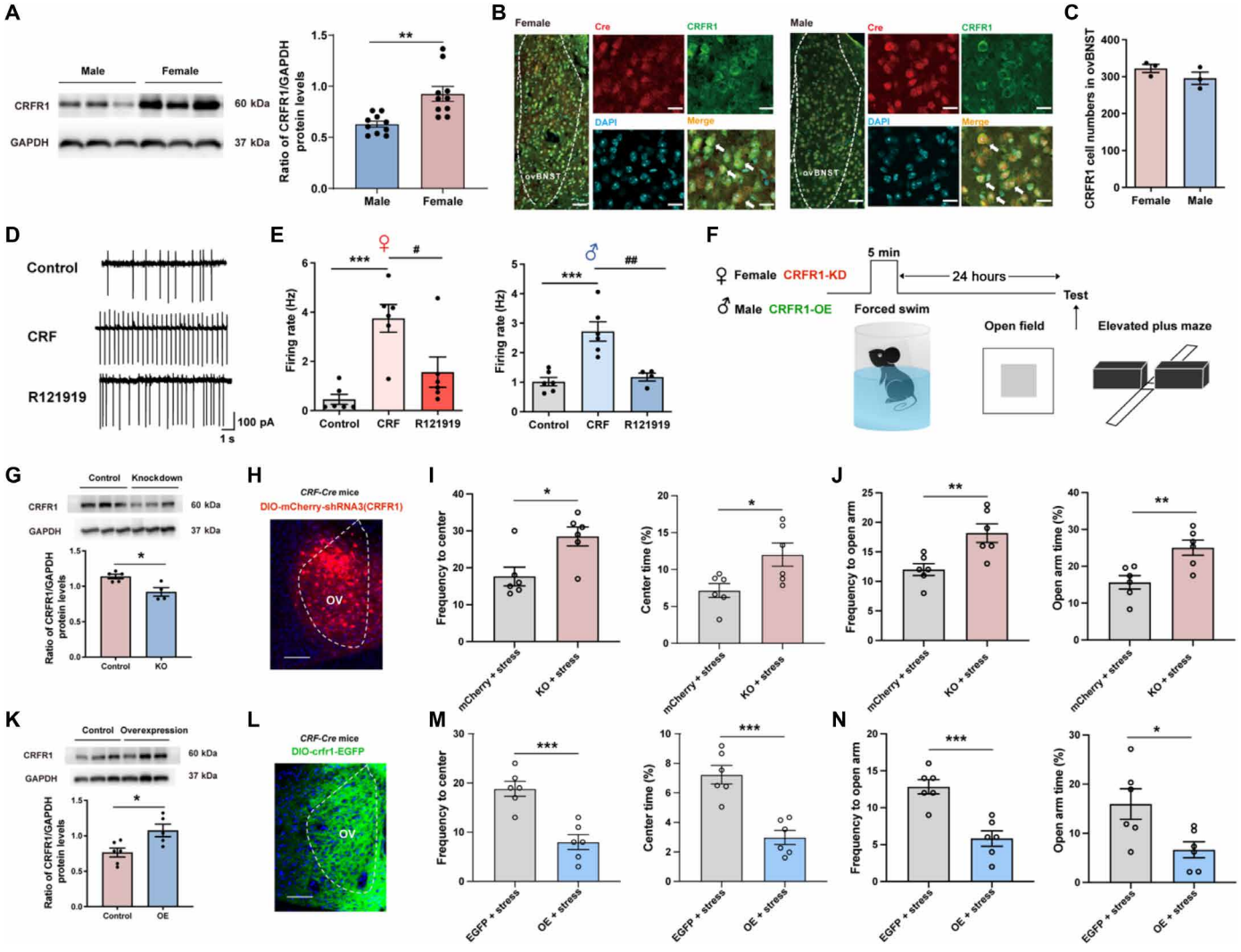


**Fig. 6. CRFR1 mediates the CRF-induced excitation of ovBNST CRF neurons during stress and contributes to the female-biased expression of stress-induced anxiety.** (**A**) Left: Representative image showing expression of CRFR1 in control mice. Right: Quantification of the expression of CRFR1 in female and male mice (**$P < 0.01$, unpaired *t* test). (**B**) Immunofluorescence staining of CRFR1 (green) and Cre (red) in the ovBNST of female (left) and male (right) *CRF-Cre* mice. Scale bars, 50 μm. (**C**) Quantification of CRFR1 neurons number between the ovBNST of female and male mice (unpaired *t* test). (**D**) Representative firing rate of ovBNST CRF neurons at base condition, after CRF perfusion and following R121919 perfusion. (**E**) Quantification of the firing rate of ovBNST CRF neurons at base condition, after CRF perfusion and following R121919 condition (***$P < 0.001$, $^{\#}P < 0.05$, and $^{\#\#}P < 0.01$, one-way ANOVA and post hoc test). (**F**) Experimental timeline. (**G**) Representative image (up) and quantification (down) of the expression of CRFR1 in control and CRFR1 knockdown female mice (*$P < 0.05$, unpaired *t* test). (**H**) Representative image showing expression of DIO-mCherry-shRNA3(CRFR1) in ovBNST. Scale bar, 200 μm. (**I** and **J**) Quantification of frequency to center zone and percentage time spent in the center zone of OFT (I), as well as quantification of frequency to open arm and percentage time spent in the open arm of EPM (J) in female mice (*$P < 0.05$ and **$P < 0.01$, Student's *t* test). (**K**) Representative image (up) and quantification (down) of the expression of CRFR1 in control and CRFR1 overexpression female mice (*$P < 0.05$, unpaired *t* test). (**L**) Representative image showing expression of DIO-crfr1-EGFP in ovBNST. Scale bar, 200 μm. (**M** and **N**) Quantification of frequency to center zone and percentage time spent in the center zone of OFT (M), as well as quantification of frequency to open arm and percentage time spent in the open arm of EPM (N) in male mice (*$P < 0.05$ and ***$P < 0.001$, Student's *t* test). GAPDH, glyceraldehyde phosphate dehydrogenase. KD, knock down; KO, knock out; OE, over expression.

ovBNST CRF neurons in female mice (Fig. 6, G and H) and expressed the virus DIO-crfr1-EGFP into the ovBNST to elevate the CRFR1 expression in ovBNST CRF neurons in male mice (Fig. 6, K and L). The results showed that decreasing the CRFR1 level in ovBNST CRF neurons in females could reverse the stress-induced anxiety-like behaviors with increased frequency and percentage of open arm entries on the EPM and center zone entries on the OFT, that is to make female behavior more like male (Fig. 6, I and J). Conversely, elevating the CRFR1 level in ovBNST CRF neurons in males could promote the expression of stress-induced anxiety-like behaviors with reduced frequency and percentage of open arm entries on the EPM and center zone entries on the OFT, that is to make males behave like females (Fig. 6, M and N). The above results indicated that CRFR1 could mediate the CRF-induced excitation of ovBNST CRF neurons and contribute to the female-biased susceptibility to anxiety.

## DISCUSSION

Recent studies have provided strong evidence that differences in hormonal balance and brain circuitry between males and females could contribute to sexually dimorphic behaviors in neuroscience (*13*, *28*), especially in anxiety-like behaviors (*29*). However, the specific mechanisms that are responsible for sex biases in the occurrence of acute stress-induced anxiety are largely not clear. In this study, our findings identify a sex-specific CRF network within the ovBNST encoding the female-biased susceptibility to anxiety. We established a female-biased stress paradigm that female mice display higher susceptibility to anxiety than male mice after acute exposure to forced swimming stress. Then, we found that amygdaloid CRF afferents in the ovBNST are involved in the stress and anxiety but unexpectedly do not show sex differences. However, the overall CRF release in ovBNST during stress shows female-biased pattern, and stress exposure induces hyperexcitation of ovBNST CRF neurons in female but not male mice in both in vitro and in vivo tests. Moreover, optogenetic modulation to exchange the activation pattern of ovBNST CRF neurons during stress between female and male mice could reverse their susceptibility to stress-induced anxiety. Last, CRFR1 could mediate the CRF-induced excitation of ovBNST CRF neurons, and prestress expression of CRFR1 in ovBNST neurons in female mice significantly outnumbers those in male mice. Specific knockdown of the CRFR1 expression in female ovBNST CRF neurons or overexpression of the CRFR1 in male ovBNST CRF neurons could reverse their susceptibility to stress-induced anxiety. Our results provide mechanistic support for previously unidentified therapeutics across sex in CRF-dependent anxiety.

For many years, a large number of studies have eliminated female animals in experiments to avoid the impact of ovarian hormone fluctuation on behaviors, which ultimately result in missing crucial information related to behavioral and physiological features of females (*30*). This problem deserves special attention in studies related to anxiety, which twice as many women were diagnosed with as men (*2*). Although there have already been reports of sexual different brain circuitry underlying stress-related behaviors, the specific mechanisms responsible for female biases in the occurrence of anxiety are largely not clear. To explore this issue, a useful model for exhibiting sex-specific susceptibility to anxiety is particularly important. It has been reported that chronic physical and social isolation stress could induce sex-specific consequences in anxiety-related behaviors where chronic social isolation stress induced social withdrawal in females but not in males, and female mice are more prone to develop anxiety-like behaviors than male mice following chronic variable stress (*21*, *22*). However, the effect of acute stress on female-biased anxiety remains uncovered. Therefore, we introduced forced swimming as an acute strong stress (*23*), which is also easily applied to mice. We succeeded to induce female-biased vulnerability to anxiety after exposure to forced swimming stress, such that female mice develop anxiety-like behaviors 24 hours after 5-min forced swimming stress exposure, while male mice remain resilient. Nevertheless, with sufficient stress, both sexes exhibited behavioral susceptibility, rendering this a useful model for studying sex difference susceptibility to anxiety. It has been reported that ovarian hormones could affect anxiety behaviors where female rodents show more anxiety-like behaviors during estrus than diestrus (*31*). However, we found here that forced swimming-induced stress paradigm is insusceptible to estrus cycles, indicating that the behavioral sex difference might be encoded by something other than hormones. We identify the crucial role for the CRF system on female-biased susceptibility to anxiety after exposure to the forced swimming.

To our knowledge, the CRF system in the brain has a well-established role in regulating the stress response and anxiety-like behaviors (*10*, *32*). In addition to hypothalamic-pituitary-adrenal axis (*33*), the CRF system expressed in the limbic brain is also involved in stress-induced anxiety-like behaviors, including the amygdala (*34*), BNST (*14*), globus pallidus (*35*), and so on. In particular, CRF-containing afferents from the CeA that project to the ovBNST (*13*) are believed to be key mediators in the expression of anxiety in both male and female rodents (*14*, *36*). Although there were no sexual differences in the anatomy of CeA-ovBNST CRF pathway as well as their role in stress-induced susceptibility to anxiety, we unexpectedly found that the overall CRF release in ovBNST during stress shows female-biased pattern. The pattern for CRF release was consistent with the pattern for CRF neuronal activities, where female mice showed continuous CRF release and activation of CRF neurons in ovBNST, but male mice showed transient CRF release and activation of CRF neurons in ovBNST. These results indicate that in addition to CeA CRF afferents, there might be other presynaptic release of CRF in ovBNST or local release of CRF from ovBNST CRF interneurons, which lead to the sexual different CRF release pattern in ovBNST during stress.

The action of CRF on neuronal excitability in the ovBNST is believed to be critical for the expression of stress-induced anxiety (*14*). Despite previous studies have reported that ovBNST CRF neurons are involved in distress-related circuits and could produce aversive effects in both female and male mice (*37*, *38*), it has not been demonstrated whether there are preexisting differences in ovBNST CRF neural activities driving sex differential vulnerability to anxiety. In our study, in in vitro electrophysiological tests, we found that CRF exposure could induce hyperexcitation of ovBNST CRF neurons in female, but not male, mice. Moreover, in in vivo fiber photometry, our study consistently showed that the activation pattern of ovBNST CRF neurons during forced swimming stress is sexually different, with persistent hyperexcitation in female mice but transient in male mice. Meanwhile, optogenetic modulation to exchange the activation pattern of ovBNST CRF neurons during stress between female and male mice could reverse their susceptibility to stress-induced anxiety. Therefore, the above results suggest that CRF release during stress could induce the hyperexcitation of ovBNST CRF neurons in female mice, which underlies the female-biased expression of anxiety-like behaviors after stress.

CRF acts primarily through CRFR1, and the BNST is the critical site for CRF-dependent actions. We unexpectedly observed that the prestress expression of ovBNST CRFR1 in females significantly outnumbers that in males. It is generally acknowledged that the CRFR1 is a postsynaptic $G_s$-coupled receptor and could mediate the release of intracellular calcium from stores (*26*). To test whether CRFR1-mediated signaling is recruited during forced swimming stress and required for the female-biased expression of anxiety-like behaviors after stress, we introduced the CRFR1 antagonist R121919 and CRFR1 agonist CRF. The results showed that intra-ovBNST administration of R121919 could reduce the susceptibility to anxiety in female mice, while intra-ovBNST administration of CRF could enhance the susceptibility to anxiety in male mice. Moreover, as traditional pharmacological manipulation is a noncell type–specific method, we also specifically modulated the expression of CRFR1 in ovBNST CRF neurons. The results showed that specific knockdown

of the CRFR1 expression in female ovBNST CRF neurons or overexpression of the CRFR1 in male ovBNST CRF neurons could reverse their susceptibility to stress-induced anxiety. These findings suggest that the sexually dimorphic expression of CRFR1s in the ovBNST contributes to the female-biased susceptibility to forced swimming stress-induced anxiety. CRF receptor type 2 (CRFR2) also widely expressed in the BNST but restricted in the posteromedial aspect of the BNST and largely non-overlapped with CRFR1 (*39*, *40*). Moreover, although CRFR2 has also been reported to be located on presynaptic axon terminals of hypothalamus oxytocin neurons in the ovBNST (*41*), it is not involved in the CeA-ovBNST CRF projections. Therefore, we did not investigate the effect of CRFR2 in the ovBNST on forced swimming-induced anxiety in this study.

Last, we expect to summarize the mechanism underlying CRF-dependent anxiety in females. Our results clearly showed that the CRFR1 in the ovBNST of female mice significantly outnumbered that in male mice. Therefore, there are more CRFR1s in the ovBNST of females than males to response the CRF release in the ovBNST during stress, and the signaling cascade following CRFR1 activation is definitely stronger in females than males. Furthermore, we confirmed the previously report that the number of ovBNST CRF neurons in female mice is significantly larger than that in male mice (*18*). If CRFR1s are localized exclusively or largely in CRF neurons in the ovBNST, then more CRFR1s and more CRF neurons in the ovBNST of female mice than in male mice suggest double effects of CRF-dependent stress on female mice versus male mice. This can explain our findings that female mice were more prone than male mice in response to the forced swimming stress, if the forced swimming stress is CRF dependent. This idea is supported by a series of findings in this study. First, female anxiety-like behavior in response to forced swimming stress was reversed by intra-ovBNST infusion of CRFR1 antagonist and specific knockdown of the CRFR1 level in ovBNST CRF neurons. Second, the activation of ovBNST CRF neurons in females was persistent throughout the whole 5-min process while in males was transient for approximately 2 min. Third, our in vitro electrophysiological study showed that in base condition, ovBNST CRF neurons in male mice are more active than that in female mice with higher spontaneous and evoked action potentials. After CRF exposure, however, the increase in spontaneous and evoked action potentials are significantly more and lasted longer in female than male mice. The sEPSC frequency of ovBNST CRF neurons after CRF exposure was higher in female than male mice. Our electrophysiological study also demonstrated that CRF-induced activation of ovBNST CRF neurons could be blocked by CRFR1 antagonist, R121919. These results indicate that the activation of ovBNST CRF neurons in females during stress is CRFR1 dependent.

In the past 10 years, huge technological advances, such as optogenetics and trans-synaptic tracing strategies, have been made to allow for the cell type–specific dissection and manipulation of neural circuits in behaving animals (*42*). Moreover, scientists have gradually attached more importance to understand and treat disorders across sex in recent years, especially focusing on the female-biased emotion disorders (*28*, *43*, *44*). On the basis of previous studies, our findings further identify a sex-specific CRF network within the ovBNST encoding the female-biased susceptibility to anxiety. Moreover, hormonal influence is also an important aspect mediating sex different behaviors. There are some studies suggested that the levels of gonadal steroids in a developmentally critical period might affect the number of BNST CRF neurons in adulthood (*45*). Therefore, hormonal manipulations under castration would be a good direction to investigate the origin of sex differences in ovBNST CRF signaling, and we will try to figure it out in the following studies. We expect this study to provide knowledge about female brains and develop better treatments for CRF-dependent anxiety.

## MATERIALS AND METHODS

### Animals

CRF Cre-recombinase mice (CRF-Cre mice, strain no. 012704) were provided by J. Hu lab (ShanghaiTech University, Shanghai, China) and genotyped according to the protocols from the Jackson Laboratory. C57BL/6J mice were purchased from the Vital River Laboratory Animal Technology Co. Ltd. (Beijing, China). All male and female adult mice were housed in a 12-hour light-dark cycle environment (temperature, 20° to 25°C; humidity, 40 to 70%), with food and water provided ad libitum. All procedures were approved by the Animal Ethics and Experimentation Committee of the Qingdao University and were conducted in accordance with National Institutes of Health (NIH) Animal Care and Use Guidelines.

### Stereotactic surgeries

For experiments requiring stereotactic surgeries, adult male and female mice (8 weeks old) were deeply anesthetized with 5% isoflurane in oxygen in an induction chamber and kept at 1 to 1.5% isoflurane during surgery. Surgery was performed with a stereotaxic frame (David Kopf Instruments, Tujunga, CA). An incision was made down the midline of the scalp, and burr holes were stereotactically made on the skull.

For administration of viruses, viruses were microinjected into the targeted regions with a glass micropipette controlled by an injection pump at a rate of 30 nl/min. After infusion, the micropipette was left in place for 10 min to allow for diffusion and prevent backflow of the virus before the pipette was slowly withdrawn. Optical fibers (Inper, Hangzhou, China) were implanted 0.15 mm above the ovBNST [Anterior-Posterior (AP): +0.26 mm; Medial-Lateral (ML): +1 mm; Dorsal-Ventral (DV): −4 mm] after virus injection. Only the mice with correct locations of fiber optic cannula and viral expression are taken into analysis.

For infusion experiments, guide cannula (RWD Life Science, Shenzhen, China) were implanted and attached to the skull using dental cement. Behavioral experiments were performed 2 weeks after the surgery. Only the mice with correct locations of cannula are taken into analysis.

### Viral delivery

For fiber photometry, AAV2/9-Ef1α-DIO-GCaMP6(m)-WPRE was injected into the ovBNST (AP: +0.26 mm; ML: ±1 mm; DV: −4 mm) or CeA (AP: −1.22 mm; ML: +3 mm; DV: −4.5 mm) of *CRF-Cre* mice. For using CRF sensor to monitor the CRF release in ovBNST during stress, AAV9-hsyn-DIO-CRF2.0 was injected into the ovBNST of *CRF-Cre* mice. For in vivo optogenetic manipulations, AAV2/9-Ef1α-DIO-ChR2-mCherry, AAV2/9-Ef1α-DIO-eNpHR3.0-mCherry, or AAV2/9-Ef1α-DIO-mCherry-WPRE as a control was injected into the ovBNST of *CRF-Cre* mice. For in vivo chemogenetic manipulations, AAV2/9-Ef1α-DIO-hM3D-mCherry, AAV2/9-Ef1α-DIO-hM4D-mCherry, or AAV2/9-Ef1α-DIO-mCherry-WPRE as a control was injected into the ovBNST

or CeA of *CRF-Cre* mice. For ablation of ovBNST CRF neurons, AAV2/9- Ef1α-DIO-Caspase3 was injected into the ovBNST of *CRF-Cre* mice. For knockdown or overexpression of CRFR1 in ovBNST CRF neurons, DIO-mCherry-shRNA3(CRFR1) was injected into the ovBNST of female *CRF-Cre* mice, and DIO-crfr1-EGFP was injected into the ovBNST of male *CRF-Cre* mice. We injected 100 nl of adeno-associated viruses (AAV) per site. All AAV viruses were produced by the OBiO Technology Shanghai Corp. Ltd. (Shanghai, China), Brain Case (Shenzhen) Co. Ltd., or BrainVTA (Wuhan) Co. Ltd. and had titers of $>10^{12}$ genome copies/ml. Behavioral experiments were performed 4 weeks after the surgery.

For anterograde tracing, AAV2/1-Ef1α-DIO-EGFP-WPRE was injected into the CeA and AAV2/9-Ef1α-DIO-mCherry-WPRE into the ovBNST of CRF-Cre mice. After 5 weeks, the brains were extracted and sectioned at 30 μm on a freezing microtome. The images were collected by a digital pathology section system (Olympus, Japan). The CeA CRF neurons could be labeled with EGFP, and the labeled EGFP CeA CRF neurons could send dense terminals and trans-synaptically labeled the downstream neurons in the ovBNST. Meanwhile, ovBNST CRF neurons were labeled with mCherry. Then, the merged yellow signals indicated the part of ovBNST CRF neurons innervated by CeA CRF neurons.

### Vaginal cytology

The estrous cycle stage of female mice was identified by vaginal cytology. Cells were collected with a cotton swab moistened with saline solution, using a rolling motion against the vaginal epithelial wall, and transferred onto a slide. Slides were air-dried and stained with Wright-Giemsa Stain solution (G1020, Solarbio). Slides were rinsed with double distilled water ($ddH_2O$) and air-dried before four estrous stages assessment under a bright field microscope.

### Forced swimming stress

Mice were placed in a beaker (12 cm in diameter by 30 cm in height) filled with water up to 20 cm (between 23° and 28°C) for 3, 5, or 10 min, respectively, and then returned to their home cage. For drug administration, 15 min before the forced swimming stress, CRF (1 μg in 0.3 μl per site, MedChemExpress) or R121919 (1 μg in 0.3 μl per site, MedChemExpress) was infused through the internal cannula inserted in the guide cannula, while control animals received saline solution. For in vivo optogenetic manipulations, yellow light was delivered as constant illumination, whereas blue light was delivered as a train of 20-Hz, 5-ms pulses during the forced swimming stress.

### Behavioral assessments

#### *Open-field test*

A white square box (40 cm by 40 cm by 35 cm, a 20 cm by 20 cm square center was defined as "center" in analysis) was used as open-field box. Mice were placed in the center of the open arena and monitored for 10 min. The light intensity in the center zone of open field was ~10 lux. All behaviors were videotaped and analyzed with Etho Vision (Noldus Information Technology).

#### *Elevated plus maze*

An EPM (55 cm above the floor) with two opposing open arms (30 cm by 8 cm) and two opposing closed arms (30 cm by 8 cm by 15 cm) was used to measure the anxiety level. Mice were placed in the center of an EPM, facing an open arm, and allowed to explore for 6 min. The light intensity in the center zone of EPM was ~15 lux. All behaviors were videotaped and analyzed with Etho Vision (Noldus Information Technology).

### In vivo fiber photometry

Following AAV2/9-Ef1α-DIO-GCaMP6(m)-WPRE virus injection, an optical fiber was placed in a ceramic ferrule and inserted toward the ovBNST through the craniotomy. The start of fiber photometry of calcium signals was 1 week after implantation surgery. The fiber photometry system (Nanjing Thinkertech) was used as our previous methods (*42*). Photometry data were exported to MATLAB Mat files for further analysis. We derived the values of fluorescence change ($\Delta F/F$) by calculating $(F - F0)/F0$.

### In vitro electrophysiology

To obtain acute coronal ovBNST slices (300 μm), mice were decapitated under isoflurane anesthesia, and the brain was quickly removed and submerged in artificial cerebrospinal fluid (ACSF; 119 mM NaCl, 2.5 mM KCl, 2.5 mM $CaCl_2$, 1 mM $NaH_2PO_4$, 1.3 mM $MgSO_4$, 26.2 $NaHCO_3$, and 11 D-glucose) at 4°C and saturated with 95% $O_2$/5% $CO_2$ as previous studies (*42*, *46*). Patch pipettes (electrode resistances, 4 to 8 megohm) were pulled from glass capillaries on a two-stage puller. For recording spiking properties, the patch pipette solution contained 35 mM K-gluconate, 110 mM KCl, 10 mM Hepes, 2 mM $MgCl_2$, 2 mM $Na_2$–adenosine triphosphate, and 10 mM EGTA (pH 7.4). Action potential firing rates were measured by injecting depolarizing current steps (15 to 115 pA, 1 s). sEPSC was measured in voltage-clamp configuration ($V_{hold} = -70$ mV) using cesium-based internal solution in ACSF containing 2 mM $Ca^{2+}$, 1 mM $Mg^{2+}$, and 0.01 bicuculline.

### Immunofluorescence staining

After the mice were perfused with saline and 4% paraformaldehyde (PFA), the brains were extracted and fixed in 4% PFA for 4 to 6 hours and then immersed in 20 and 30% sucrose at 4°C. Each brain was sectioned at 30 μm on a freezing microtome and collected in 0.01 M phosphate-buffered saline (PBS). The sections were washed three times in 0.01 M PBS for 10 min at room temperature. Sections were then incubated in blocking solution made of phosphate-buffered saline with Tween detergent (PBST) with 5% donkey serum for 1 hour at room temperature. Sections were next incubated in primary antibodies goat anti-CRFR1 (1:200; Abcam, ab77686) or rabbit anti-Cre recombinase (1:500; Abcam, ab190177) overnight at 4°C. After washing three times with 0.01 M PBS, the sections were incubated with species-specific secondary antibodies Alexa Fluor 488 or 555 (1:500; Invitrogen, A48258) for 2 hours at room temperature. Sections were then washed three times for 10 min in 0.01 M PBS. Last, the sections were mounted with antifade mounting medium, and images were collected by a digital pathology section system (Olympus, Japan).

### Western blot

Protein samples were loaded in 12% SDS–polyacrylamide gel electrophoresis, transferred to a polyvinylidene fluoride membrane, and immunobloted with anti-CRFR1 antibodies (1:500; ab77686, Abcam) and anti–glyceraldehyde phosphate dehydrogenase antibodies (1:3000; abs830030, Absin). Then, horseradish peroxidase–conjugated anti-goat immunoglobulin G (IgG) and anti-mouse IgG secondary antibodies were incubated against each primary antibody. Western

blot bands were imaged by the enhanced chemiluminescence Western blotting detection system (Millipore Corp., Billerica, MA, USA). ImageJ software (NIH Image, Bethesda, MD, USA) was used to analyze the bands.

### Statistics

Statistical analysis was conducted with GraphPad Prism software with appropriate inferential methods as indicated in the figure legends. The number of experimental replicates ($n$) is indicated in figures and refers to the number of experimental subjects used and independently treated in each experimental condition. Data are presented as the mean ± SEM. Student's $t$ test was used to compare two groups. One-way analysis of variance (ANOVA) was used, and the Bonferroni test was performed for multiple comparisons. No statistical methods were used to predetermine the sample size or to randomize. Differences were considered significant when $P < 0.05$.

## Supplementary Materials

**This PDF file includes:**

Figs. S1 to S9

## REFERENCES AND NOTES


1. COVID-19 Mental Disorders Collaborators, Global prevalence and burden of depressive and anxiety disorders in 204 countries and territories in 2020 due to the COVID-19 pandemic. *Lancet* **398**, 1700–1712 (2021).
2. B. W. Penninx, D. S. Pine, E. A. Holmes, A. Reif, Anxiety disorders. *Lancet* **397**, 914–927 (2021).
3. M. G. Craske, M. B. Stein, Anxiety. *Lancet* **388**, 3048–3059 (2016).
4. D. A. Bangasser, A. Cuarenta, Sex differences in anxiety and depression: Circuits and mechanisms. *Nat. Rev. Neurosci.* **22**, 674–684 (2021).
5. A. K. Beery, I. Zucker, Sex bias in neuroscience and biomedical research. *Neurosci. Biobehav. Rev.* **35**, 565–572 (2011).
6. R. M. Shansky, Are hormones a "female problem" for animal research? *Science* **364**, 825–826 (2019).
7. R. Apps, P. Strata, Neuronal circuits for fear and anxiety - the missing link. *Nat. Rev. Neurosci.* **16**, 642 (2015).
8. B. Xue, X. Zhang, Y. Wang, Bench to bedside: Multiple facets of cannabinoid control in epilepsy. *Neurochem. Int.* **141**, 104898 (2020).
9. C. Tao, G. W. Zhang, J. J. Huang, Z. Li, H. W. Tao, L. I. Zhang, The medial preoptic area mediates depressive-like behaviors induced by ovarian hormone withdrawal through distinct GABAergic projections. *Nat. Neurosci.* **26**, 1529–1540 (2023).
10. J. M. Deussing, A. Chen, The corticotropin-releasing factor family: Physiology of the stress response. *Physiol. Rev.* **98**, 2225–2286 (2018).
11. P. Hu, J. Liu, I. Maita, C. Kwok, E. Gu, M. M. Gergues, F. Kelada, M. Phan, J. N. Zhou, D. F. Swaab, Z. P. Pang, P. J. Lucassen, T. A. Roepke, B. A. Samuels, Chronic stress induces maladaptive behaviors by activating corticotropin-releasing hormone signaling in the mouse oval bed nucleus of the stria terminalis. *J. Neurosci.* **40**, 2519–2537 (2020).
12. S. Y. Kim, A. Adhikari, S. Y. Lee, J. H. Marshel, C. K. Kim, C. S. Mallory, M. Lo, S. Pak, J. Mattis, B. K. Lim, R. C. Malenka, M. R. Warden, R. Neve, K. M. Tye, K. Deisseroth, Diverging neural pathways assemble a behavioural state from separable features in anxiety. *Nature* **496**, 219–223 (2013).
13. G. de Guglielmo, M. Kallupi, M. B. Pomrenze, E. Crawford, S. Simpson, P. Schweitzer, G. F. Koob, R. O. Messing, O. George, Inactivation of a CRF-dependent amygdalofugal pathway reverses addiction-like behaviors in alcohol-dependent rats. *Nat. Commun.* **10**, 1238 (2019).
14. M. B. Pomrenze, J. Tovar-Diaz, A. Blasio, R. Maiya, S. M. Giovanetti, K. Lei, H. Morikawa, F. W. Hopf, R. O. Messing, A corticotropin releasing factor network in the extended amygdala for anxiety. *J. Neurosci.* **39**, 1030–1043 (2019).
15. J. Dabrowska, R. Hazra, J. D. Guo, S. Dewitt, D. G. Rainnie, Central CRF neurons are not created equal: Phenotypic differences in CRF-containing neurons of the rat paraventricular hypothalamus and the bed nucleus of the stria terminalis. *Front. Neurosci.* **7**, 156 (2013).
16. J. N. Zhou, M. A. Hofman, L. J. Gooren, D. F. Swaab, A sex difference in the human brain and its relation to transsexuality. *Nature* **378**, 68–70 (1995).
17. M. Hines, F. C. Davis, A. Coquelin, R. W. Goy, R. A. Gorski, Sexually dimorphic regions in the medial preoptic area and the bed nucleus of the stria terminalis of the guinea pig brain: A description and an investigation of their relationship to gonadal steroids in adulthood. *J. Neurosci.* **5**, 40–47 (1985).
18. K. Uchida, H. Otsuka, M. Morishita, S. Tsukahara, T. Sato, K. Sakimura, K. Itoi, Female-biased sexual dimorphism of corticotropin-releasing factor neurons in the bed nucleus of the stria terminalis. *Biol. Sex Differ.* **10**, 6 (2019).
19. L. Sterrenburg, B. Gaszner, J. Boerrigter, L. Santbergen, M. Bramini, E. W. Roubos, B. W. Peeters, T. Kozicz, Sex-dependent and differential responses to acute restraint stress of corticotropin-releasing factor-producing neurons in the rat paraventricular nucleus, central amygdala, and bed nucleus of the stria terminalis. *J. Neurosci. Res.* **90**, 179–192 (2012).
20. T. Funabashi, M. Kawaguchi, M. Furuta, A. Fukushima, F. Kimura, Exposure to bisphenol A during gestation and lactation causes loss of sex difference in corticotropin-releasing hormone-immunoreactive neurons in the bed nucleus of the stria terminalis of rats. *Psychoneuroendocrinology* **29**, 475–485 (2004).
21. T. Tan, W. Wang, T. Liu, P. Zhong, M. Conrow-Graham, X. Tian, Z. Yan, Neural circuits and activity dynamics underlying sex-specific effects of chronic social isolation stress. *Cell Rep.* **34**, 108874 (2021).
22. J. Muir, Y. C. Tse, E. S. Iyer, J. Biris, V. Cvetkovska, J. Lopez, R. C. Bagot, Ventral hippocampal afferents to nucleus accumbens encode both latent vulnerability and stress-induced susceptibility. *Biol. Psychiatry* **88**, 843–854 (2020).
23. S. H. Sunwoo, J. S. Lee, S. Bae, Y. J. Shin, C. S. Kim, S. Y. Joo, H. S. Choi, M. Suh, S. W. Kim, Y. J. Choi, T. I. Kim, Chronic and acute stress monitoring by electrophysiological signals from adrenal gland. *Proc. Natl. Acad. Sci. U.S.A.* **116**, 1146–1151 (2019).
24. J. Muir, Z. S. Lorsch, C. Ramakrishnan, K. Deisseroth, E. J. Nestler, E. S. Calipari, R. C. Bagot, In vivo fiber photometry reveals signature of future stress susceptibility in nucleus accumbens. *Neuropsychopharmacology* **43**, 255–263 (2018).
25. H. Wang, T. Qian, Y. Zhao, Y. Zhuo, C. Wu, T. Osakada, P. Chen, Z. Chen, H. Ren, Y. Yan, L. Geng, S. Fu, L. Mei, G. Li, L. Wu, Y. Jiang, W. Qian, L. Zhang, W. Peng, M. Xu, J. Hu, M. Jiang, L. Chen, C. Tang, Y. Zhu, D. Lin, J. N. Zhou, Y. Li, A tool kit of highly selective and sensitive genetically encoded neuropeptide sensors. *Science* **382**, eabq8173 (2023).
26. A. C. Riegel, J. T. Williams, CRF facilitates calcium release from intracellular stores in midbrain dopamine neurons. *Neuron* **57**, 559–570 (2008).
27. A. Iemolo, A. Blasio, S. A. S. Cyr, F. Jiang, K. C. Rice, V. Sabino, P. Cottone, CRF-CRF1 receptor system in the central and basolateral nuclei of the amygdala differentially mediates excessive eating of palatable food. *Neuropsychopharmacology* **38**, 2456–2466 (2013).
28. T. M. Gruene, K. Flick, A. Stefano, S. D. Shea, R. M. Shansky, Sexually divergent expression of active and passive conditioned fear responses in rats. *eLife* **4**, (2015).
29. K. Li, M. Nakajima, I. Ibanez-Tallon, N. Heintz, A cortical circuit for sexually dimorphic oxytocin-dependent anxiety behaviors. *Cell* **167**, 60–72 e11 (2016).
30. J. A. Clayton, F. S. Collins, Policy: NIH to balance sex in cell and animal studies. *Nature* **509**, 282–283 (2014).
31. K. G. Bath, J. Chuang, J. L. Spencer-Segal, D. Amso, M. Altemus, B. S. McEwen, F. S. Lee, Variant brain-derived neurotrophic factor (Valine66Methionine) polymorphism contributes to developmental and estrous stage-specific expression of anxiety-like behavior in female mice. *Biol. Psychiatry* **72**, 499–504 (2012).
32. M. J. Henckens, J. M. Deussing, A. Chen, Region-specific roles of the corticotropin-releasing factor-urocortin system in stress. *Nat. Rev. Neurosci.* **17**, 636–651 (2016).
33. Y. Wang, H. Xu, X. Zhang, Breakthrough in structural and functional dissection of the hypothalamo-neurohypophysial system. *Neurosci. Bull.* **37**, 1087–1089 (2021).
34. C. Jiang, X. Yang, G. He, F. Wang, Z. Wang, W. Xu, Y. Mao, L. Ma, F. Wang, $CRH^{CeA \rightarrow VTA}$ inputs inhibit the positive ensembles to induce negative effect of opiate withdrawal. *Mol. Psychiatry* **26**, 6170–6186 (2021).
35. Y. Sztainberg, Y. Kuperman, N. Justice, A. Chen, An anxiolytic role for CRF receptor type 1 in the globus pallidus. *J. Neurosci.* **31**, 17416–17424 (2011).
36. J. G. Oberlander, L. P. Henderson, Corticotropin-releasing factor modulation of forebrain GABAergic transmission has a pivotal role in the expression of anabolic steroid-induced anxiety in the female mouse. *Neuropsychopharmacology* **37**, 1483–1499 (2012).
37. C. A. Marcinkiewcz, C. M. Mazzone, G. D'Agostino, L. R. Halladay, J. A. Hardaway, J. F. DiBerto, M. Navarro, N. Burnham, C. Cristiano, C. E. Dorrier, G. J. Tipton, C. Ramakrishnan, T. Kozicz, K. Deisseroth, T. E. Thiele, Z. A. McElligott, A. Holmes, L. K. Heisler, T. L. Kash, Serotonin engages an anxiety and fear-promoting circuit in the extended amygdala. *Nature* **537**, 97–101 (2016).
38. H. M. Baumgartner, J. Schulkin, K. C. Berridge, Activating corticotropin-releasing factor systems in the nucleus accumbens, amygdala, and bed nucleus of stria terminalis: Incentive motivation or aversive motivation? *Biol. Psychiatry* **89**, 1162–1175 (2021).
39. K. Van Pett, V. Viau, J. C. Bittencourt, R. K. Chan, H. Y. Li, C. Arias, G. S. Prins, M. Perrin, W. Vale, P. E. Sawchenko, Distribution of mRNAs encoding CRF receptors in brain and pituitary of rat and mouse. *J. Comp. Neurol.* **428**, 191–212 (2000).
40. M. Henckens, Y. Printz, U. Shamgar, J. Dine, M. Lebow, Y. Drori, C. Kuehne, A. Kolarz, M. Eder, J. M. Deussing, N. J. Justice, O. Yizhar, A. Chen, CRF receptor type 2 neurons in the posterior bed nucleus of the stria terminalis critically contribute to stress recovery. *Mol. Psychiatry* **22**, 1691–1700 (2017).

41. D. Martinon, J. Dabrowska, Corticotropin-releasing factor receptors modulate oxytocin release in the dorsolateral bed nucleus of the stria terminalis (BNST) in male rats. *Front. Neurosci.* **12**, 183 (2018).
42. Y. Wang, Y. Wang, C. Xu, S. Wang, N. Tan, C. Chen, L. Chen, X. Wu, F. Fei, H. Cheng, W. Lin, Y. Qi, B. Chen, J. Liang, J. Zhao, Z. Xu, Y. Guo, S. Zhang, X. Li, Y. Zhou, S. Duan, Z. Chen, Direct septum-hippocampus cholinergic circuit attenuates seizure through driving somatostatin inhibition. *Biol. Psychiatry* **87**, 843–856 (2020).
43. S. Lima, N. Sousa, P. Patricio, L. Pinto, The underestimated sex: A review on female animal models of depression. *Neurosci. Biobehav. Rev.* **133**, 104498 (2022).
44. A. V. Williams, C. J. Pena, S. Ramos-Maciel, A. Laman-Maharg, E. Ordonez-Sanchez, M. Britton, B. Durbin-Johnson, M. Settles, R. Hao, S. Yokoyama, C. Xu, P. X. Luo, T. Dwyer, S. Bhela, A. M. Black, B. Labonte, R. A. Serafini, A. Ruiz, R. L. Neve, V. Zachariou, E. J. Nestler, B. C. Trainor, Comparative transcriptional analyses in the nucleus accumbens identifies RGS2 as a key mediator of depression-related behavior. *Biol. Psychiatry* **92**, 942–951 (2022).
45. A. Fukushima, M. Furuta, F. Kimura, T. Akema, T. Funabashi, Testosterone exposure during the critical period decreases corticotropin-releasing hormone-immunoreactive neurons in the bed nucleus of the stria terminalis of female rats. *Neurosci. Lett.* **534**, 64–68 (2013).
46. W. C. Oh, G. Rodriguez, D. Asede, K. Jung, I. W. Hwang, R. Ogelman, M. M. Bolton, H. B. Kwon, Dysregulation of the mesoprefrontal dopamine circuit mediates an early-life stress-induced synaptic imbalance in the prefrontal cortex. *Cell Rep.* **35**, 109074 (2021).

**Acknowledgments**
**Funding:** X.Z. is supported by the STI2030-Major Projects grant 2021ZD0203000 (2021ZD0203002) and the National Natural Science Foundation of China grant (82090033 and 81830035). Y.W. is supported by the National Natural Science Foundation of China grant (82003729) and Natural Science Foundation of Shandong Province (ZR2020QH357). **Author contributions:** Conceptualization: Y.W. and X.Z. Methodology: Y.W., N.Z., Y.M., and X.Z. Investigation: N.Z., S.Z., Y.M., Z.X., and B.X. Validation: Y.M., B.X., S.Z., and Y.W. Visualization: Y.D., Q.W., N.Z., and Y.W. Formal analysis: Y.M., Z.X., N.Z., S.Z., and Y.W. Data curation: Y.W. Software: Y.W. Supervision: Y.W. and X.Z. Writing—original draft: N.Z. and Y.W. Writing—review and editing: Y.W., X.Z., and H.X. Resources: Y.W. and X.Z. Funding acquisition: Y.W. and X.Z. Project administration: Y.W. and X.Z. **Competing interests:** The authors declare that they have no competing interests. **Data and materials availability:** All data needed to evaluate the conclusions in the paper are present in the paper and/or the Supplementary Materials.

Submitted 18 September 2023
Accepted 9 April 2024
Published 10 May 2024
10.1126/sciadv.adk7636